Mitochondrial control of calcium-channel gating: A mechanism for sustained signaling and transcriptional activation in T lymphocytes

Markus Hoth*, Donald C. Button, and Richard S. Lewis†

Department of Molecular and Cellular Physiology, Stanford University School of Medicine, Stanford, CA 94305-5426

Edited by Richard W. Tsien, Stanford University School of Medicine, Stanford, CA, and approved July 7, 2000 (received for review March 31, 2000)

In addition to their well-known functions in cellular energy transduction, mitochondria play an important role in modulating the amplitude and time course of intracellular Ca^{2+} signals. In many cells, mitochondria act as Ca^{2+} buffers by taking up and releasing Ca^{2+}, but this simple buffering action by itself often cannot explain the organelle's effects on Ca^{2+} signaling dynamics. Here we describe the functional interaction of mitochondria with store-operated Ca^{2+} channels in T lymphocytes as a mechanism of mitochondrial Ca^{2+} signaling. In Jurkat T cells with functional mitochondria, prolonged depletion of Ca^{2+} stores causes sustained activation of the store-operated Ca^{2+} current, I_{CRAC} (CRAC, Ca^{2+} release-activated Ca^{2+}). Inhibition of mitochondrial Ca^{2+} uptake by compounds that dissipate the intramitochondrial potential unmasks Ca^{2+}-dependent inactivation of I_{CRAC}. Thus, functional mitochondria are required to maintain CRAC-channel activity, most likely by preventing local Ca^{2+} accumulation near sites that govern channel inactivation. In cells stimulated through the T-cell antigen receptor, acute blockade of mitochondrial Ca^{2+} uptake inhibits the nuclear translocation of the transcription factor NFAT in parallel with CRAC channel activity and $[Ca^{2+}]_i$ elevation, indicating a functional link between mitochondrial regulation of I_{CRAC} and T-cell activation. These results demonstrate a role for mitochondria in controlling Ca^{2+} channel activity and signal transmission from the plasma membrane to the nucleus.

Mitochondria are becoming widely recognized as multifunctional organelles that are essential not only for cellular energy transduction but also for pathways of Ca^{2+} signaling, homeostasis, and cell death (1–7). As Ca^{2+} signaling organelles, they can rapidly take up and slowly release large amounts of Ca^{2+}, enabling them not only to protect cells against cytosolic Ca^{2+} overload under pathophysiological conditions but also to shape and prolong physiological Ca^{2+} signals (1, 2, 8, 9).

Recent evidence suggests that mitochondria can also modulate the flux of Ca^{2+} across cell membranes. In a variety of nonexcitable cells, mitochondria have been shown to influence signals generated by Ca^{2+} release from the endoplasmic reticulum (ER), presumably through intimate interactions with the inositol 1,4,5-trisphosphate (IP_3) receptor (1, 4–7, 10, 11). In T lymphocytes, functional mitochondria act to sustain store-operated Ca^{2+} entry after prolonged depletion of intracellular Ca^{2+} stores (12). These examples show clearly how mitochondria may extend their influence on Ca^{2+} signaling by modulating Ca^{2+} transport pathways; however, the mechanisms underlying these phenomena are unknown. Mitochondria could alter Ca^{2+} channel activity itself or they could alter indirectly net Ca^{2+} fluxes by regulating Ca^{2+}-ATPases or by regulating the K^+ or Cl^- channels that set the driving force for Ca^{2+} entry. Furthermore, these effects in principle could be mediated by changes in local or global cell $[Ca^{2+}]_i$ or by changes in the ATP/ADP ratio, both of which are known to affect the function of IP_3 receptors (13) and store-operated Ca^{2+} channels (14–18). In addition, the physiological significance of these phenomena, if any, has not been demonstrated clearly in any system.

In this study, we examine the interaction of mitochondria with store-operated Ca^{2+} channels in T lymphocytes. Antigenic stimulation of T cells triggers intracellular Ca^{2+} release by IP_3 and the consequent opening of Ca^{2+} release-activated Ca^{2+} (CRAC) channels that in turn generate the prolonged elevation of cytosolic Ca^{2+} ($[Ca^{2+}]_i$) required for T-cell activation (19–21). Using whole-cell and perforated-patch recording techniques, we find that mitochondria prevent the inactivation of CRAC channels that results from prolonged Ca^{2+} influx. Moreover, after stimulation through the T-cell antigen receptor, mitochondrial inhibition reduces the $[Ca^{2+}]_i$ signal and in parallel inhibits the nuclear import of NFAT, a critical transcription factor for T-cell activation (22, 23). The results show that mitochondria regulate an ion channel, identify the mechanism for their interaction, and illustrate implications for downstream cellular events.

Materials and Methods

Cell Culture and Solutions. Jurkat cell clone E6–1 [American Type Culture Collection, Rockville, MD (ATCC 1378)] and a parental diphtheria toxin-resistant Jurkat clone (21) were grown in culture medium consisting of RPMI 1640 supplemented with 10% FCS and penicillin–streptomycin (21). Normal Ringer's solution contained (in mM): 155 NaCl, 4.5 KCl, 2 $CaCl_2$, 1 $MgCl_2$, 10 D-glucose, and 5 Hepes (pH 7.4 with NaOH). $CaCl_2$ was replaced by $MgCl_2$ in the 0-Ca^{2+} Ringer's solution. The standard pipette solution for whole-cell patch-clamp recordings contained (in mM): 140 cesium aspartate, 2 $MgCl_2$, 0.66 $CaCl_2$, 1.2 EGTA ($[Ca^{2+}]_{free} \approx 5$ nM), 0.1 indo-1 pentapotassium salt, and 10 Hepes (pH 7.2 with CsOH). The pipette solution for perforated-patch recordings contained (in mM): 115 Cs aspartate, 5 $MgCl_2$, 1 $CaCl_2$, 10 NaCl, 10 Hepes (pH 7.2 with CsOH), and nystatin (200–300 μg/ml, diluted 1:500 from a DMSO stock solution made daily). Reagents include thapsigargin (TG, LC Laboratories, Woburn, MA), carbonyl cyanide *m*-chlorophenylhydrazone (CCCP; Sigma), antimycin A1 (Sigma), and oligomycin (Sigma). OKT3 ascites was a generous gift from Gerald Crabtree (Stanford University, Stanford, CA).

Combined Patch-Clamp and $[Ca^{2+}]_i$ Measurements. Patch pipettes were pulled from 100-μl capillaries, coated with Sylgard, and fire polished. Membrane currents were recorded at 22–25°C with an

This paper was submitted directly (Track II) to the PNAS office.

Abbreviations: CCCP, carbonyl cyanide *m*-chlorophenylhydrazone; ER, endoplasmic reticulum; EGFP, enhanced green fluorescent protein; I_{CRAC}, calcium release-activated calcium current; NFAT, nuclear factor of activated T cells; TG, thapsigargin; CRAC, Ca^{2+} release-activated Ca^{2+}.

*Present address: Department of Physiology, University of Saarland, D-66421 Homburg, Germany.

†To whom reprint requests should be addressed. E-mail: rslewis@leland.stanford.edu.

The publication costs of this article were defrayed in part by page charge payment. This article must therefore be hereby marked "*advertisement*" in accordance with 18 U.S.C. §1734 solely to indicate this fact.

Article published online before print: *Proc. Natl. Acad. Sci. USA*, 10.1073/pnas.180143997. Article and publication date are at www.pnas.org/cgi/doi/10.1073/pnas.180143997

Axopatch 200 amplifier (Axon Instruments, Foster City, CA), filtered at 1.5 kHz, and digitized at a sampling rate of 5 kHz using an ITC-16 interface (Instrutech, Port Washington, NY). All voltages were corrected for a liquid junction potential of −12 mV between internal solutions and the bath solution. Pipette and cell capacitance were canceled electronically at the beginning of each experiment. All data were corrected for leak currents collected in 0-Ca^{2+} Ringer's solution. Series resistance in perforated-patch recordings was minimized by using low-resistance (2–3 MΩ) wide-angled pipettes backfilled with freshly made nystatin solution. The average series resistance stabilized at a value of 34 ± 11 MΩ (n = 19) within 3–5 min of forming the pipette-membrane seal (seal resistance was usually >10 GΩ). Two methods were used to deplete fully intracellular Ca^{2+} stores before perforated-patch recordings: (*i*) cells were preincubated for 5–8 min in 0-Ca^{2+} Ringer's containing 1 μM TG and incubated another 4–7 min after seal formation to allow the series resistance to stabilize; or (*ii*) seals were formed in 0.5 mM Ca^{2+} Ringer's (Ca^{2+} was reduced to prevent a sometimes large $[Ca^{2+}]_i$ rise at the time of seal formation) and incubated subsequently for 10 min in 0-Ca^{2+} + TG. In whole-cell recordings, seals were made in 0.5 mM Ca^{2+} Ringer's solution and after breaking in cells were incubated in 0-Ca^{2+} Ringer's + 1 μM TG for 3–4 min to deplete internal Ca^{2+} stores. A dual-photomultiplier-based fluorescence microscope was used to monitor $[Ca^{2+}]_i$ during patch-clamp recordings (15). Cells were loaded with 100 μM indo-1 pentapotassium salt (Molecular Probes) through the whole-cell recording pipette or by incubation with 1 μM indo-1/AM in medium for 20 min at 22–25°C in perforated-patch experiments (achieving a final intracellular concentration of 50–100 μM). All data are given as mean ± SEM (number of experiments).

Combined NFAT-EGFP and $[Ca^{2+}]_i$ Measurements. Jurkat cells were transfected by electroporation (21) with an expression construct in which a CMV promoter drives expression of an EGFP-tagged NFATc1 protein (enhanced GFP fused to the C terminus of NFATc1; construct kindly provided by S. Park and G. Crabtree, Stanford University). For measurements on cells transiently expressing NFATc1-EGFP (Fig. 3 *B* and *C*), cells with high levels of EGFP fluorescence (but omitting the brightest 5% of all cells) were collected by flow cytometry 24–30 h after transfection. In addition, a nonclonal population of Jurkat cells stably expressing NFATc1-EGFP (Fig. 3*D*) was isolated through several rounds of sorting for abundant EGFP expression. Both sets of cells were loaded with 1 μM fura-2/AM in culture medium for 20–30 min at 22–25°C, and $[Ca^{2+}]_i$ was measured in single cells with a video microscope setup described previously (12, 21). Cells were illuminated for 267 ms at 350 ± 7 and 380 ± 7 nm (to excite fura-2) and 485 ± 11 nm (to excite EGFP) every 5–10 sec (Chroma Technology, Brattleboro, VT). Emission at 535 nm ± 22.5 nm was collected with an intensified CCD camera (Hamamatsu, Bridgewater, NJ) and digitized using a VideoProbe image processor (ETM Systems, Irvine, CA). For each time point, global cell $[Ca^{2+}]$ was calculated from the 350/380 ratio as described (12, 21), whereas EGFP fluorescence was analyzed spatially in one of two ways. For the TG experiments (Fig. 3 *B* and *C*), nuclear EGFP intensity was measured within a small area in the middle of the nucleus, and the cytosolic intensity was calculated from the average of several extranuclear areas of similar size around the cell perimeter. Only cells that did not move during the 500-s observation period were analyzed. In the anti-CD3 experiments (Fig. 3*D*), only nuclear NFATc1-EGFP intensity was measured to facilitate analysis of a much larger number of cells. Nuclear location was confirmed in several experiments by staining with Hoechst 33258 (not shown). Extent of translocation is expressed as the percent change in the EGFP signal relative to the intensity at time 0 without background correction. These measurements underestimate the true extent of translocation, as some degree of crossover between the nuclear and cytoplasmic EGFP signals is expected from out-of-focus fluorescence. All data are given as mean ± SEM (number of experiments).

Results

Mitochondrial Inhibitors Evoke CRAC-Channel Inactivation. CRAC current (I_{CRAC}) was measured in Jurkat T cells using the noninvasive perforated-patch technique, with no exogenous cytosolic Ca^{2+} buffers applied other than a small amount of indo-1/AM for the purpose of measuring $[Ca^{2+}]_i$. The ER Ca^{2+} store was depleted by treatment for 3 min with 1 μM TG in Ca^{2+}-free Ringer's solution. The subsequent addition of 2 mM Ca^{2+} to the bath induced a small sustained inward current (average current density of −0.44 ± 0.21 pA/pF, n = 8) accompanied by an increase in $[Ca^{2+}]_i$ to a supramicromolar level (Fig. 1*A*). The current was identified as I_{CRAC} by its dependence on store depletion and extracellular Ca^{2+} and by its inwardly rectifying current-voltage relation (Fig. 1*B*) (19, 24). Fig. 1 *C* and *D* show the results from a similar experiment conducted in the presence of 1 μM CCCP, a lipophilic protonophore that blocks mitochondrial Ca^{2+} uptake by dissipating the negative mitochondrial potential (8, 9). With CCCP present, I_{CRAC} inactivated with a time constant of ≈40 s after Ca^{2+} readdition, declining to a steady-state level of ≈50% within 100 s (Fig. 1*C*). The shape and reversal potential of the current–voltage relation remained constant during the experiment (Fig. 1*D*), showing that the current's decline was not caused by induction of an outward current, but rather by a reduction of I_{CRAC}. The degree of inactivation in CCCP-treated cells relative to control did not correlate with the peak current density, which on average was not affected significantly by CCCP (peak current density of −0.59 ± 0.25 pA/pF in 8 CCCP-treated cells; −0.44 ± 0.21 pA/pF in 8 control cells). As a consequence of the decrease in I_{CRAC}, $[Ca^{2+}]_i$ also declined from a peak of >1 μM to a lower plateau. We obtained similar results with antimycin A1 and oligomycin, structurally unrelated compounds that depolarize mitochondria and inhibit their uptake of Ca^{2+} through a different mechanism involving inhibition of electron transport and the $F_o - F_1$ ATPase (see summary in Fig. 1*E*). Again, no correlation was found between peak current density and degree of inactivation.

The Mechanism of Coupling Between Mitochondria and CRAC Channels. The slow decline of I_{CRAC} in the presence of mitochondrial inhibitors is similar in kinetics and extent to the slow Ca^{2+}-dependent inactivation of I_{CRAC} that has been described in whole-cell recordings from Jurkat (15) and RBL cells (16). Slow inactivation occurs under conditions in which store refilling is prevented by TG and $[Ca^{2+}]_i$ is allowed to rise (i.e., in the presence of low exogenous Ca^{2+} buffering in the recording pipette). To test whether mitochondrial inhibitors promote this type of inactivation, we conducted a series of whole-cell recordings starting with the ionic conditions of our original study (15). After establishing the whole-cell configuration with a weakly Ca^{2+}-buffered internal solution (see Fig. 2 legend), each cell was treated for 3–4 min in 0-Ca^{2+} Ringer's solution containing 1 μM TG to achieve complete store depletion. As reported previously (15), readdition of Ca^{2+} to the cell evoked large CRAC currents that rapidly overcame the low intracellular buffering capacity, increasing $[Ca^{2+}]_i$ to supramicromolar levels and causing I_{CRAC} to inactivate by ≈50% within 100 sec (Fig. 2 *A* and *B*). This result contrasts markedly with the results of perforated-patch recordings in which little or no inactivation was seen (Fig. 1*A*). Because inhibition of mitochondrial Ca^{2+} uptake leads to inactivation in the perforated-patch configuration, we reasoned that the similar inactivation seen in whole-cell recordings might have resulted

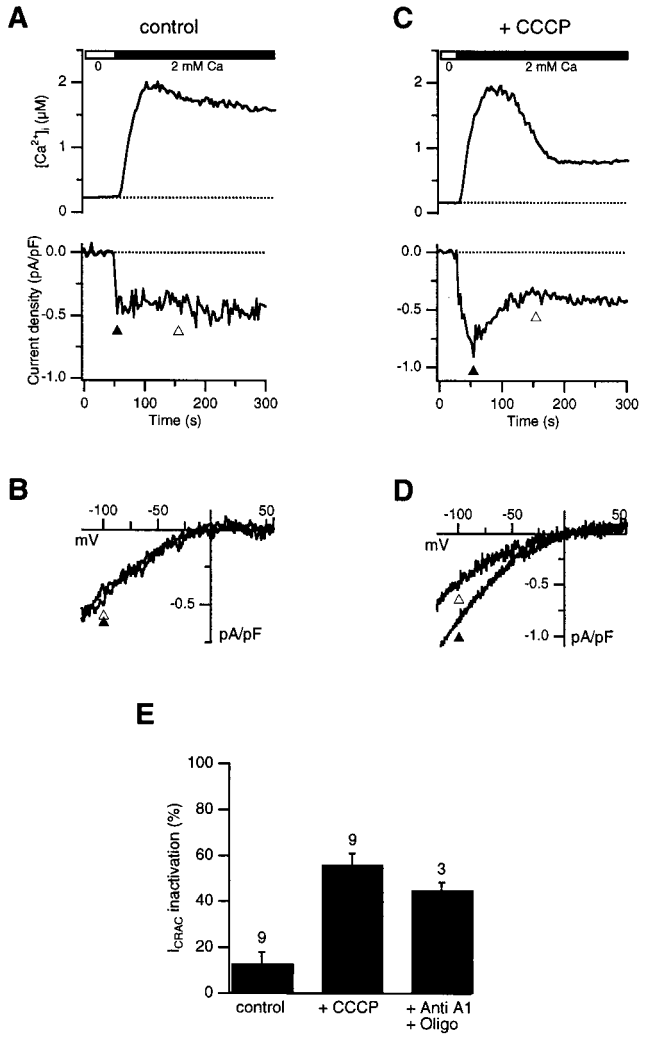

Fig. 1. Inhibition of mitochondrial Ca^{2+} uptake evokes CRAC channel inactivation. I_{CRAC} and $[Ca^{2+}]_i$ were measured in parallel using the perforated patch-clamp technique in the absence (*A, B*) or presence (*C, D*) of 1 μM CCCP (present throughout the experiments). After irreversible store depletion by TG in 0-Ca^{2+} Ringer's solution (see *Materials and Methods*), 2 mM Ca^{2+} was added to measure I_{CRAC}. A voltage step to -120 mV followed by a voltage ramp from -120 mV to + 60 mV was applied every 2 s from the holding potential (-40 mV). Current density at -100 mV is plotted in *A* and *C* (*Lower*), and leak-corrected ramp currents collected at the times indicated by the triangles are shown in *B* and *D*. (*E*) I_{CRAC} inactivation is plotted as the current measured 100 s after the peak (open triangles in *A* and *C*) relative to the peak current amplitude (solid triangles in *A* and *C*). 1 μM CCCP or 2 μM antimycin A1 + 1 μM oligomycin increase I_{CRAC} inactivation significantly relative to control (unpaired Student's *t* test, $P < 0.007$). The number of cells for each condition is indicated.

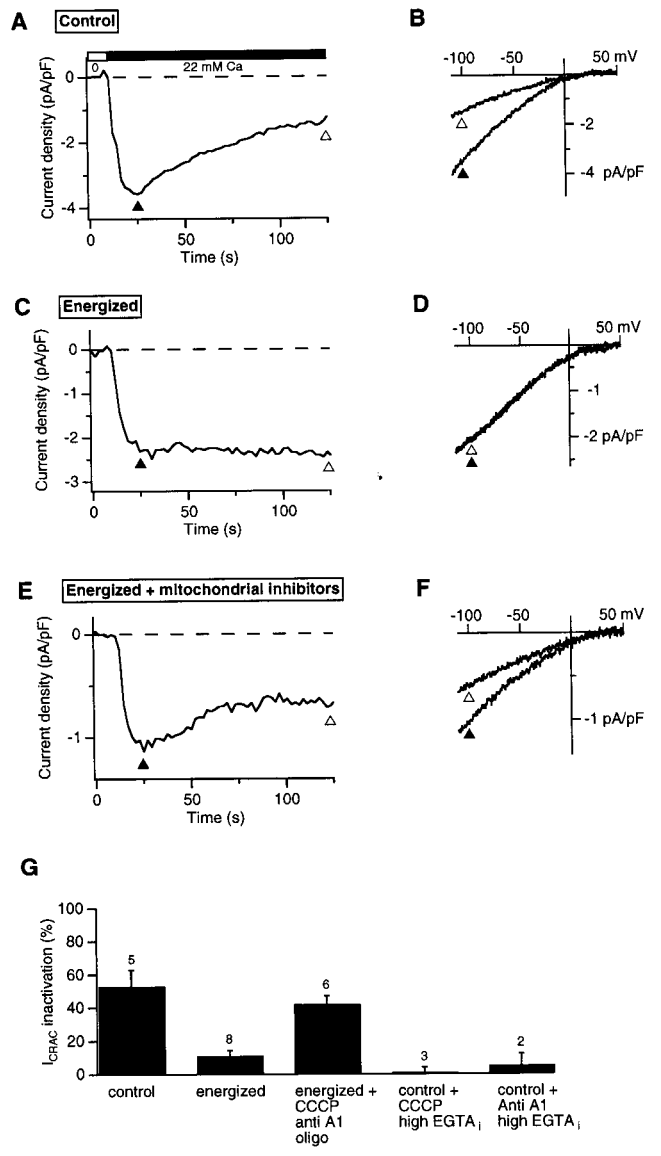

Fig. 2. Energized mitochondria prevent Ca^{2+}-dependent inactivation of CRAC channels. I_{CRAC} was measured in whole-cell recordings with 1.2 mM EGTA in the recording pipette. Stimulus protocol was identical to that used in Fig. 1. (*A*) I_{CRAC} measured at -100 mV before and after addition of 22 mM Ca^{2+} using the standard whole-cell internal solution (see *Materials and Methods*). (*B*) Leak-corrected ramp currents collected at the times indicated by the triangles in *A*. (*C, D*) I_{CRAC} recorded as in *A* and *B* with the addition of 2.5 mM malic acid/2.5 mM Na pyruvate/1 mM NaH_2PO_4/5 mM MgATP/0.5 mM Tris·GTP to the recording pipette to support mitochondrial function (''energized'' conditions). (*E, F*) I_{CRAC} recorded as in *C* and *D* with addition of 1 μM CCCP/2 μM antimycin A1/1 μM oligomycin to the bath. (*G*) CRAC channel inactivation under various conditions measured as described in Fig. 1. Inactivation under energized conditions or in the presence of 12 mM internal EGTA (last two bars) was significantly less than under the other conditions shown (unpaired Student's *t* test, $P < 0.007$). The number of cells for each condition is indicated.

from a loss of mitochondrial function, possibly because of washout of oxidative substrates. To test this hypothesis, we supplemented the pipette solution with several compounds to help maintain the mitochondrial potential (9, 25): 2.5 mM malic acid/2.5 mM Na pyruvate/1 mM NaH_2PO_4/5 mM MgATP/0.5 mM Tris·GTP. Under these ''energized'' whole-cell conditions, CRAC channel activity was sustained (Fig. 2 *C* and *D*). To rule out the possibility that the added compounds prevent inactivation through a nonmitochondrial mechanism, energized cells were treated with CCCP, antimycin A1, and oligomycin (Fig. 2 *E* and *F*). The inhibitors clearly unmask inactivation despite the presence of the mitochondrial substrates, supporting the conclusion that the energy state of the mitochondria controls the extent of Ca^{2+}-dependent I_{CRAC} inactivation.

A likely explanation for the effect of mitochondria on I_{CRAC} is that by taking up Ca^{2+}, they reduce the free $[Ca^{2+}]_i$ at sites that trigger inactivation. This idea is consistent with the results summarized in Figs. 1*E* and 2*G* showing that I_{CRAC} inactivates when mitochondrial Ca^{2+} uptake is impaired (e.g., with CCCP

or antimycin + oligomycin) but does not inactivate when mitochondrial Ca^{2+} uptake can occur (e.g., in perforated-patch configuration or under "energized" whole-cell conditions). Moreover, addition of 12 mM EGTA intracellularly to prevent the rise in $[Ca^{2+}]_i$ (15) also prevents I_{CRAC} inactivation caused by mitochondrial inhibitors, demonstrating that the inactivation is in fact Ca^{2+}-dependent (Fig. 2*G*). The notion that mitochondria may reduce $[Ca^{2+}]_i$ locally near CRAC channels is supported by previous findings that Ca^{2+} uptake by mitochondria in T cells and other cells is known to occur rapidly and with high capacity (12, 26), and that mitochondria are close enough to apparently sense local Ca^{2+} gradients near open CRAC channels in T cells (12). Two Ca^{2+}-independent explanations for the effects of mitochondrial inhibitors were also considered. The most obvious is that these poisons might diminish I_{CRAC} by depleting cellular ATP (17, 18). Such a mechanism is unlikely to explain our results for several reasons. First, I_{CRAC} inactivated in the presence of the inhibitors despite the presence of 5 mM ATP supplied through the whole-cell recording pipette (Fig. 2*E*). Second, luciferase measurements on Jurkat cell suspensions indicated that intracellular [ATP] was stable over a period of 30 min in cells treated with TG and either antimycin A1 or CCCP in the presence of oligomycin (data not shown); this result is consistent with the known ability of glycolysis to supply the energy needs of tumor cells (27). Third, oligomycin did not diminish the effect of CCCP or antimycin A1 on inactivation (data not shown), even though it prevents ATP consumption resulting from reverse-mode operation of the $F_o - F_1$ ATPase (28). A second alternative explanation we have considered is that the mitochondrial inhibitors may block I_{CRAC} through a side effect unrelated to their effects on mitochondria. This possibility is also unlikely, however, as CRAC channel inactivation in the presence of CCCP or antimycin is prevented fully by the 12 mM EGTA added intracellularly (Fig. 2*G*). This result confirms that the mitochondrial inhibitors unmask Ca^{2+}-dependent inactivation of I_{CRAC} rather than inhibiting the channels directly.

Physiological Consequences of Mitochondrial Regulation of CRAC Channels. Because sustained elevation of $[Ca^{2+}]_i$ plays a crucial role in T-cell activation, it is important to determine how mitochondrial regulation of I_{CRAC} may influence downstream effector pathways. We examined the acute effects of mitochondrial inhibitors on the nuclear translocation of NFATc1, a critical transcription factor in T cells whose translocation to the nucleus is triggered by the Ca^{2+}-dependent phosphatase calcineurin (22, 23). Cytosolic $[Ca^{2+}]$ and the localization of an NFATc1-EGFP chimera were measured simultaneously in Jurkat cells using video microscopy (Fig. 3*A*). As shown in Fig. 3*B*, addition of Ca^{2+} to TG-treated cells caused a sustained $[Ca^{2+}]_i$ rise and a progressive accumulation of NFATc1-EGFP in the nucleus mirrored by a decrease in cytosolic intensity, indicating nuclear import. In contrast, Ca^{2+} readdition in the presence of CCCP resulted in CRAC-channel inactivation and an early decline in $[Ca^{2+}]_i$ from its initial peak level (Fig. 3*C*). Although the initial rate for nuclear translocation of NFATc1-EGFP was similar to that of control cells, accumulation ceased shortly after the fall in $[Ca^{2+}]_i$. The average increase in nuclear EGFP intensity 500 s after Ca^{2+} readdition was reduced by about half in CCCP-treated cells ($29 \pm 4\%, n = 25$) compared with control ($59 \pm 6\%$, $n = 40$; unpaired Student's t test, $P < 0.01$). CCCP apparently does not interfere directly with nuclear import because normal nuclear translocation of NFATc1-EGFP was observed in those CCCP-treated cells (6 of 25) in which Ca^{2+} readdition evoked normal sustained $[Ca^{2+}]_i$ elevation.

One concern about the use of TG as the Ca^{2+}-mobilizing stimulus in these experiments is that blockade of SERCA pumps may obscure the contributions of Ca^{2+} sequestration by the ER, possibly leading to an overestimate of the role of mitochondria. For this reason, we also tested the ability of mitochondria to promote NFAT translocation under more physiological conditions. Cells were treated at 37°C with OKT3, an anti-CD3 monoclonal antibody that activates T cells by crosslinking the T-cell receptor complex (29). As shown in Fig. 3*D*, mitochondrial inhibitors attenuated the plateau phase of the $[Ca^{2+}]_i$ response by ≈50%, from 437 ± 88 nM in control cells (7 experiments on 527 cells) to 214 ± 58 nM in cells treated with 1 μM CCCP with or without 1 μM antimycin A1 + 1 μM oligomycin (6 experiments on 486 cells; unpaired Student's t test, $P < 0.001$). Mitochondrial inhibition also impaired the nuclear translocation of NFATc1-EGFP measured in the same cells. After a brief phase of accumulation during the initial $[Ca^{2+}]_i$ rise, nuclear import slowed dramatically in the presence of CCCP (Fig. 3*D*). After 15 min of stimulation with OKT3, nuclear levels of NFATc1-EGFP increased significantly more in control cells (25 ± 7%) than in cells treated with CCCP ± antimycin A1/oligomycin (15 ± 4%; unpaired Student's t test, $P < 0.01$), consistent with the sustained elevated plateau in $[Ca^{2+}]_i$. Thus, mitochondria enhance the activation of NFAT even when ER Ca^{2+} uptake systems are operational, suggesting that the ability of mitochondria to prevent I_{CRAC} inactivation may serve to optimize Ca^{2+}-dependent transcriptional events *in vivo*.

Discussion

This study identifies store-operated Ca^{2+} channels as a target for mitochondrial modulation and describes the mechanism and a functional consequence of the interaction. The regulation of Ca^{2+} channel activity by mitochondria enables mitochondria to have a more profound impact on Ca^{2+} signaling and downstream signaling cascades than would be possible through simple Ca^{2+} buffering effects alone. Although mitochondrial inhibition of Ca^{2+}-channel inactivation has been proposed previously for ligand-gated (30), voltage-gated (28), and store-operated Ca^{2+} channels (12), and therefore might be a widespread phenomenon, the present study represents the first experimental test of this idea. Functional interactions between mitochondria and intracellular Ca^{2+} channels have also been inferred from the effects of mitochondrial inhibitors on Ca^{2+} release from the ER (10) or the propagation of cytosolic Ca^{2+} waves (1, 6, 7, 31–33). These effects have been attributed to changes in Ca^{2+} feedback on IP_3 receptors in the ER, but this hypothesis has been difficult to test directly because of the inaccessibility of IP_3 receptors in intact cells.

The functional interaction between mitochondria and CRAC channels is mediated through the control of Ca^{2+}-dependent I_{CRAC} inactivation. Mitochondria probably produce these effects by taking up Ca^{2+} and locally reducing its concentration near sites that govern inactivation rather than by reducing $[Ca^{2+}]_i$ globally, as mitochondrial inhibitors initiate the inactivation process at a time when global $[Ca^{2+}]_i$ is similar to that of control cells (e.g., compare Fig. 1 *A* and *C*). Local accumulation of Ca^{2+} may also help explain why I_{CRAC} inactivation in the presence of CCCP persists even after the global $[Ca^{2+}]_i$ has declined (Fig. 1*C*); alternatively, prolonged inhibition of I_{CRAC} could result from a slow rate of recovery from inactivation. We cannot distinguish between these two possibilities at present. A physical basis for local interactions is indicated by the close proximity of mitochondria to CRAC channels; in electron micrographs of Jurkat cells, the majority of mitochondrial profiles lie within 500 nm of the plasma membrane (M.H., J. Buchanan, and R.L., unpublished data), similar to the intimate physical coupling between mitochondria and the ER reported in other cell types (5–7). Controlling Ca^{2+} channel activity and the resultant cytosolic Ca^{2+} signals through the localization, abundance, and metabolic state of mitochondria may therefore be a general cell biological mechanism for tuning Ca^{2+} signals and subsequent cell responses. In this context, it is intriguing that mitochondrial

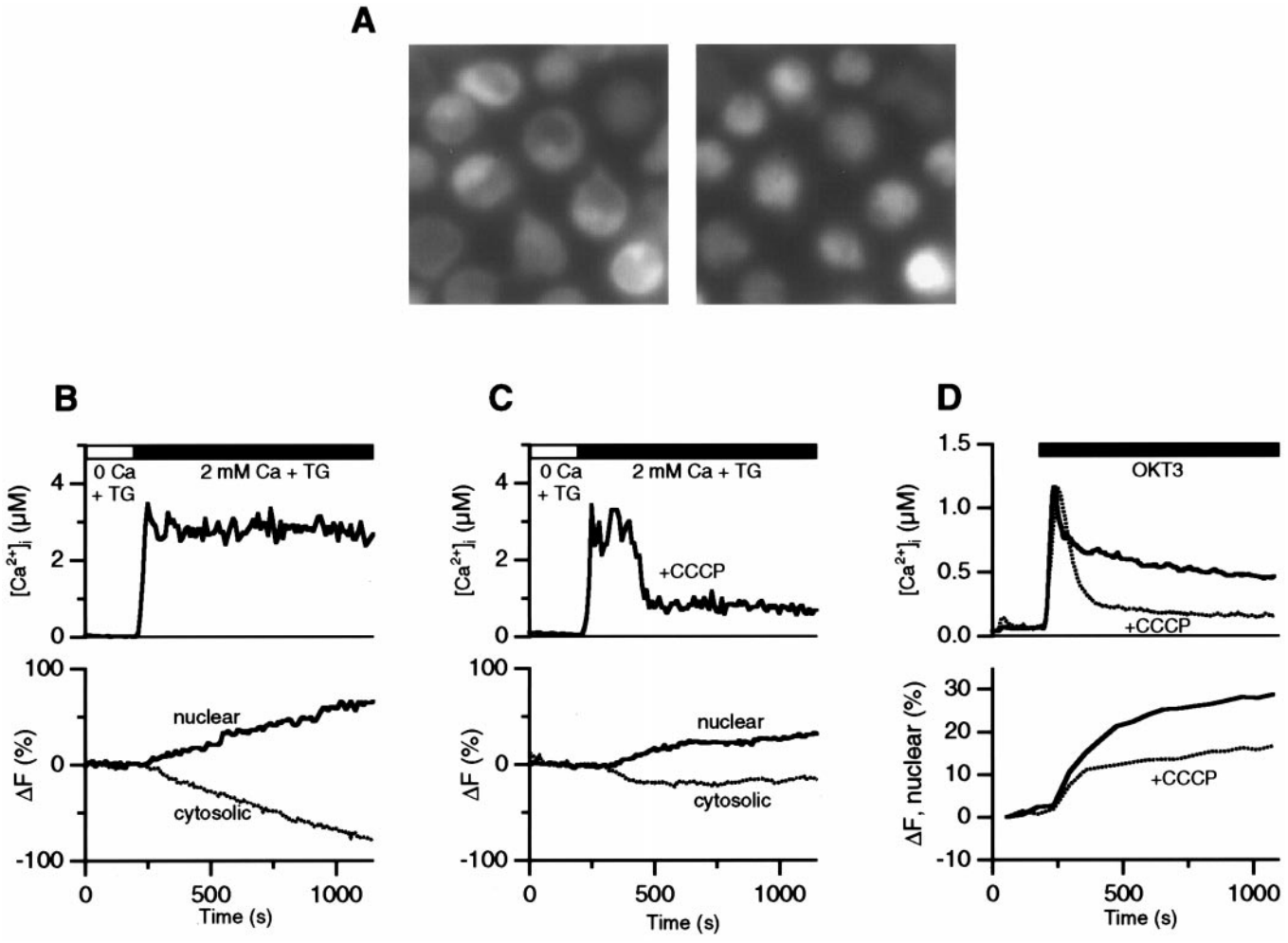

Fig. 3. Mitochondria are necessary for sustained Ca^{2+} signaling and NFAT translocation. $[Ca^{2+}]_i$ and EGFP fluorescence were measured in parallel in fura-2-loaded Jurkat cells expressing NFATc1-EGFP. (*A*) Images of NFATc1-EGFP fluorescence are shown for cells before (*Left*) or 10 min after stimulation with OKT3 (*Right*; 1:75 ascites). In unstimulated cells, NFATc1-EGFP is mostly cytosolic, and OKT3 elicits extensive translocation of NFATc1-EGFP to the nucleus. (*B, C*) $[Ca^{2+}]_i$ and EGFP fluorescence measured in the absence (*B*) or presence (*C*) of 1 μM CCCP in single cells at room temperature. After depletion of Ca^{2+} stores for 10 min in 0-Ca^{2+} + 1 μM TG, 2 mM Ca^{2+} was readded as indicated. (*D*) $[Ca^{2+}]_i$ and nuclear NFATc1-EGFP intensity in OKT3-stimulated cells at 37°C. A maximally effective concentration of OKT3 (ascites diluted 1:75) was added to the cells as indicated under control conditions (solid trace) or in the presence of 1 μM CCCP (dotted trace). Each trace is an average of three experiments performed on a single day comprising a total of 151 (control) and 146 (+CCCP) cells.

activity increases severalfold during the first few days of T cell activation (34). Thus, increased resistance to I_{CRAC} inactivation, together with increased expression of CRAC channels (35) and Ca^{2+}-activated K^+ channels (36), may contribute to the enhancement of Ca^{2+} signaling observed during this time period (37).

In a previous study of intact single T cells not under voltage clamp, mitochondrial inhibitors were found to reduce store-operated Ca^{2+} entry by increasing the likelihood of abrupt transitions from a high rate of Ca^{2+} influx to a low rate (12). These transitions were more rapid than the decreases in $[Ca^{2+}]_i$ we observe in voltage-clamped cells under otherwise similar conditions (compare Fig. 1*B* with figure 9C of ref. 12). One possible explanation for this difference is that in unclamped cells, slow inactivation of I_{CRAC} causes Ca^{2+}-activated K^+ channels to deactivate, leading to membrane depolarization. The ensuing reduction in the driving force for Ca^{2+} entry would further deactivate I_{KCa} and accelerate the transition from high to low $[Ca^{2+}]_i$.

As shown in this study, one important consequence of mitochondrial regulation of CRAC channels in T cells is to enable the sustained elevation of $[Ca^{2+}]_i$ that is required to drive nuclear translocation of NFAT. Maintained nuclear localization of NFAT is an essential prerequisite for the expression of interleukin-2 and other T-cell activation genes after exposure to antigen (22, 23). Thus, the close communication between mitochondria and CRAC channels may be important for optimizing early transcriptional events. Furthermore, these interactions are expected to have additional effects on cell signaling and metabolism, such as strengthening the link between CRAC channel activation and enhancement of ATP generation (3, 38, 39) and expanding the role of mitochondria as a pathway for Ca^{2+} redistribution from entry sites to other locations within the cell. An important goal for the future will be to determine how the appropriate coupling of mitochondria to CRAC channels is controlled, and how it contributes to setting the stimulation threshold for T cell activation and other downstream signaling events.

The authors thank Nat Blair for assistance with NFAT-EGFP experiments, Chris Fanger for helpful discussions, and Sang Ho Park and Gerald Crabtree for the NFATc1-EGFP construct and OKT3 ascites. This work was supported by postdoctoral fellowships from Boehringer Ingelheim Fonds and the Human Frontier Science Program (M.H.) and by the National Institutes of Health (R.S.L.).

1. Duchen, M. R. (1999) *J. Physiol. (London)* **516,** 1–17.
2. Gunter, T. E., Gunter, K. K., Sheu, S. S. & Gavin, C. E. (1994) *Am. J. Physiol.* **267,** C313–C339.
3. Hajnóczky, G., Robb-Gaspers, L. D., Seitz, M. B. & Thomas, A. P. (1995) *Cell* **82,** 415–424.
4. Rizzuto, R., Brini, M., Murgia, M. & Pozzan, T. (1993) *Science* **262,** 744–747.
5. Rizzuto, R., Pinton, P., Carrington, W., Fay, F. S., Fogarty, K. E., Lifshitz, L. M., Tuft, R. A. & Pozzan, T. (1998) *Science* **280,** 1763–1766.
6. Jouaville, L. S., Ichas, F., Holmuhamedov, E. L., Camacho, P. & Lechleiter, J. D. (1995) *Nature (London)* **377,** 438–441.
7. Simpson, P. B. & Russell, J. T. (1996) *J. Biol. Chem.* **271,** 33493–33501.
8. Thayer, S. A. & Miller, R. J. (1990) *J. Physiol. (London)* **425,** 85–115.
9. Babcock, D. F., Herrington, J., Goodwin, P. C., Park, Y. B. & Hille, B. (1997) *J. Cell Biol.* **136,** 833–844.
10. Hajnóczky, G., Hager, R. & Thomas, A. P. (1999) *J. Biol. Chem.* **274,** 14157–14162.
11. Duchen, M. R., Leyssens, A. & Crompton, M. (1998) *J. Cell Biol.* **142,** 975–988.
12. Hoth, M., Fanger, C. M. & Lewis, R. S. (1997) *J. Cell Biol.* **137,** 633–648.
13. Bezprozvanny, I. & Ehrlich, B. E. (1995) *J. Membr. Biol.* **145,** 205–216.
14. Parekh, A. B. & Penner, R. (1997) *Physiol. Rev.* **77,** 901–930.
15. Zweifach, A. & Lewis, R. S. (1995) *J. Biol. Chem.* **270,** 14445–14451.
16. Parekh, A. B. (1998) *J. Biol. Chem.* **273,** 14925–14932.
17. Gamberucci, A., Innocenti, B., Fulceri, R., Banhegyi, G., Giunti, R., Pozzan, T. & Benedetti, A. (1994) *J. Biol. Chem.* **269,** 23597–23602.
18. Innocenti, B., Pozzan, T. & Fasolato, C. (1996) *J. Biol. Chem.* **271,** 8582–8587.
19. Zweifach, A. & Lewis, R. S. (1993) *Proc. Natl. Acad. Sci. USA* **90,** 6295–6299.
20. Partiseti, M., Le Deist, F., Hivroz, C., Fischer, A., Korn, H. & Choquet, D. (1994) *J. Biol. Chem.* **269,** 32327–32335.
21. Fanger, C. M., Hoth, M., Crabtree, G. R. & Lewis, R. S. (1995) *J. Cell Biol.* **131,** 655–667.
22. Crabtree, G. R. & Clipstone, N. A. (1994) *Annu. Rev. Biochem.* **63,** 1045–1083.
23. Rao, A., Luo, C. & Hogan, P. G. (1997) *Annu. Rev. Immunol.* **15,** 707–747.
24. Hoth, M. & Penner, R. (1992) *Nature (London)* **355,** 353–356.
25. Villalba, M., Martinez-Serrano, A., Gomez-Puertas, P., Blanco, P., Borner, C., Villa, A., Casado, M., Gimenez, C., Pereira, R., Bogonez, E., *et al.* (1994) *J. Biol. Chem.* **269,** 2468–2476.
26. Sparagna, G. C., Gunter, K. K., Sheu, S. S. & Gunter, T. E. (1995) *J. Biol. Chem.* **270,** 27510–27515.
27. Pedersen, P. L. (1978) *Prog. Exp. Tumor Res.* **22,** 190–274.
28. Budd, S. L. & Nicholls, D. G. (1996) *J. Neurochem.* **66,** 403–411.
29. Weiss, A., Imboden, J., Hardy, K., Manger, B., Terhorst, C. & Stobo, J. (1986) *Ann. Rev. Immunol.* **4,** 593–619.
30. Budd, S. L. & Nicholls, D. G. (1996) *J. Neurochem.* **67,** 2282–2291.
31. Simpson, P. B., Mehotra, S., Langley, D., Sheppard, C. A. & Russell, J. T. (1998) *J. Neurosci. Res.* **52,** 672–683.
32. Boitier, E., Rea, R. & Duchen, M. R. (1999) *J. Cell Biol.* **145,** 795–808.
33. Falcke, M., Hudson, J. L., Camacho, P. & Lechleiter, J. D. (1999) *Biophys. J.* **77,** 37–44.
34. Ferlini, C., Biselli, R., Nisini, R. & Fattorossi, A. (1995) *Cytometry* **21,** 284–293.
35. Fomina, A. F., Fanger, C. M., Kozak, J. A. & Cahalan, M. D. (2000) *J. Cell Biol.*, in press.
36. Grissmer, S., Nguyen, A. N. & Cahalan, M. D. (1993) *J. Gen. Physiol.* **102,** 601–630.
37. Verheugen, J. A., Le Deist, F., Devignot, V. & Korn, H. (1997) *Cell Calcium* **21,** 1–17.
38. Robb-Gaspers, L. D., Burnett, P., Rutter, G. A., Denton, R. M., Rizzuto, R. & Thomas, A. P. (1998) *EMBO J.* **17,** 4987–5000.
39. Jouaville, L. S., Pinton, P., Bastianutto, C., Rutter, G. A. & Rizzuto, R. (1999) *Proc. Natl. Acad. Sci. USA* **96,** 13807–13812.